

# Gravitating non-Abelian cosmic strings

Antônio de Pádua Santos\* and Eugênio R. Bezerra de Mello†

*Departamento de Física, Universidade Federal da Paraíba,  
58.059-970, Caixa Postal 5.008, João Pessoa, PB, Brazil*

(Dated: January 27, 2022)

In this paper we study regular cosmic string solutions of the non-Abelian Higgs model coupled with gravity. In order to develop this analysis, we constructed a set of coupled non-linear differential equations. Because there is no closed solution for this set of equations, we solve it numerically. The solutions that we are interested in asymptote to a flat space-time with a planar angle deficit. This model under consideration present two bosonic sectors, besides the non-Abelian gauge field. The two bosonic sectors may present a direct coupling. So, we investigate the relevance of this coupling on the system, specifically in the linear energy density of the string and on the planar angle deficit. We also analyze the behaviors of these quantities as function of the energy scale where the gauge symmetry is spontaneously broken.

PACS numbers: 98.80.Cq, 11.27.+d

---

\* padua.santos@gmail.com

† emello@fisica.ufpb.br

## I. INTRODUCTION

According to the Big Bang theory, the universe has been expanding and cooling. During its early evolution, the universe has been underwent a series of phase transitions characterized by spontaneous symmetry breaking [1]. These phase transitions are important, because they provide a mechanism for the formation of topological defects such as domain walls, monopoles, cosmic string, among others [2]. In the eighties of last century the interest to cosmic strings has been increase due to the fact that they were considered candidates to provide a mechanism for the large-scale structure formation in the universe. Although the recent observations of the Cosmic Microwave Background (CMB) radiation have ruled out cosmic strings as seed for the primordial density perturbations, they are still candidates to explain a small non-Gaussianity in the cosmic microwave background and the influence on the temperature anisotropies. Such effects had origins in the gravitational fields of cosmic strings in motion [3]. In addition, astrophysical and cosmological consequences of formation of strings are emission of gravitational waves and high energy cosmic rays such as neutrinos and gamma-rays. These observational data can help to constraint the product of the Newton's constant  $G$  to the linear mass density of cosmic string,  $\mu$  [4]. These effects are generated by cosmic strings formed under inflation context<sup>1</sup> which makes the physics of cosmic strings a vast area of interest.

The first theoretical model associated with strings-like solutions was given by Nielsen and Olesen [6] by using an Abelian Higgs model lagrangian which presents a spontaneously  $U(1)$  gauge symmetry broken. These solutions were also named by **vortex**. The influence of this system on the geometry of the spacetime has been analyzed in [7, 8] many years ago, by coupling the energy-momentum tensor associated with the Nielsen and Olesen string with the Einstein equations. In these papers, static and cylindrically solutions for the matter and gauge fields and also for the metric tensor, were investigated numerically by using coupled ordinary non-linear differential equations. A few years latter the Abelian Higgs model has also investigated in [9] and [10]. The so-called (p,q) gravitating cosmic string have been analyzed numerically in [11]. In the latter, static and cylindrically solutions of the system containing two different Abelian gauge fields coupled with two bosonic sectors were investigated.

In this paper we are interested to analyze the cosmic string solution again, however, considering at this time the  $SU(2)$  non-Abelian Higgs model coupled to gravity. As it was also shown in [6], to create a non-Abelian topological stable string, it is necessary the presence of two bosonic iso-vectors coupled with the gauge field. The interaction potential should present terms with fourth powers in these bosonic fields in order to have spontaneously gauge symmetry broken. Moreover, it may contain a direct interaction between these bosonic sectors.

This paper is organized as follows: In section II we present the non-Abelian Higgs model coupled to gravity and analyze the conditions that the physical parameters contained in the potential should satisfy in order the system provides stable topological solutions. In section II A we present the ansatz for the matter and gauge fields, and for the metric tensor. The equations of motion and boundary conditions obeyed by the fields and metric tensor are presented in section III. In section IV we exhibit our numerical results for the behaviors of the fields considering different values of the relevant parameters. In this section we present a comparison of this non-Abelian system with the Abelian one. Also we investigate the behaviors of the energy density of the string and planar angle deficit, as functions of the energy scale where the  $SU(2)$  gauge symmetry is spontaneously broken and the interaction coupling between the bosonic sectors. In section V we give our conclusions and in the Appendix we present a special solution of the system that, although the corresponding configuration is not in according to stable topological configuration, it behaves as a BPS solution of the fields equations .

## II. THE MODEL

The model that we want to study is described by the following action,  $S$ :

$$S = \int d^4x \sqrt{-g} \left( \frac{1}{16\pi G} R + \mathcal{L}_m \right), \quad (1)$$

where  $R$  is the Ricci scalar,  $G$  denotes the Newton's constant and  $\mathcal{L}_m$  is the matter Lagrangian density of the non-Abelian Higgs model given by

$$\mathcal{L}_m = -\frac{1}{4} F_{\mu\nu}^a F^{\mu\nu a} + \frac{1}{2} (D_\mu \varphi^a)^2 + \frac{1}{2} (D_\mu \chi^a)^2 - V(\varphi^a, \chi^a), \quad a = 1, 2, 3. \quad (2)$$

---

<sup>1</sup> Observational consequences generated by cosmic strings can be found in [4, 5].

The field strength tensor is

$$F_{\mu\nu}^a = \partial_\mu A_\nu^a - \partial_\nu A_\mu^a + e\epsilon^{abc}A_\mu^b A_\nu^c, \quad (3)$$

with the  $SU(2)$  gauge potential  $A_\mu^b$ , and  $e$  being the gauge coupling constant. The covariant derivatives of the Higgs fields are given by [6],

$$D_\mu \varphi^a = \partial_\mu \varphi^a + e\epsilon^{abc}A_\mu^b \varphi^c, \quad (4)$$

$$D_\mu \chi^a = \partial_\mu \chi^a + e\epsilon^{abc}A_\mu^b \chi^c, \quad (5)$$

where the latin indices denote the internal gauge groups ( $a, b = 1, 2, 3$ ). The interaction potential,  $V(\varphi^a, \chi^a)$ , which we shall consider is expressed by

$$V(\varphi^a, \chi^a) = \frac{\lambda_1}{4} [(\varphi^a)^2 - \eta_1^2]^2 + \frac{\lambda_2}{4} [(\chi^a)^2 - \eta_2^2]^2 + \frac{\lambda_3}{2} [(\varphi^a)^2 - \eta_1^2] [(\chi^a)^2 - \eta_2^2], \quad (6)$$

where the  $\lambda_1$  and  $\lambda_2$  are the Higgs fields self-coupling positive constants and  $\lambda_3$  is the coupling constant between both bosonic sectors.  $\eta_1$  and  $\eta_2$  parameters correspond to energy scale where the gauge symmetry is broken. The potential above has different properties according to the sign of  $\Delta \equiv \lambda_1 \lambda_2 - \lambda_3^2$ :

- For  $\Delta > 0$ , the potential has positive value and its minimum is attained for  $(\varphi^a)^2 = \eta_1^2$  and  $(\chi^a)^2 = \eta_2^2$ .
- For  $\Delta < 0$ , these configuration becomes saddle points and two minima occur for:

$$(\varphi^a)^2 = 0, \quad (\chi^a)^2 = \eta_2^2 + \frac{\lambda_3}{\lambda_2} \eta_1^2 \quad (7)$$

and

$$(\chi^a)^2 = 0, \quad (\varphi^a)^2 = \eta_1^2 + \frac{\lambda_3}{\lambda_1} \eta_2^2. \quad (8)$$

The values of the potential for these cases are, respectively,

$$V_{min} = \frac{\eta_1^4}{4\lambda_2} \Delta \quad \text{and} \quad V_{min} = \frac{\eta_2^4}{4\lambda_1} \Delta. \quad (9)$$

Both values for  $V_{min}$  are negatives, since  $\Delta < 0$ .

### A. The Ansatz

The Euler-Lagrange equations for the Higgs and gauge fields, and the Einstein equations for the metric tensor are obtained as presented below.

First let us consider the most general, cylindrically symmetric line element invariant under boosts along z-direction. By using cylindrical coordinates, this line element is given by:

$$ds^2 = N^2(\rho)dt^2 - d\rho^2 - L^2(\rho)d\phi^2 - N^2(\rho)dz^2. \quad (10)$$

For this metric, the only non-vanishing components of the Ricci tensor,  $R_{\mu\nu}$ , are:

$$R_{tt} = -R_{zz} = \frac{NLN'' + NN'L' + L(N')^2}{L}, \quad (11)$$

$$R_{\rho\rho} = \frac{2LN'' + NL''}{NL}, \quad (12)$$

$$R_{\phi\phi} = \frac{L(2N'L' + NL'')}{N}, \quad (13)$$

where the primes denotes derivative with respect to  $\rho$ .

As to the bosonic sectors and gauge fields [12], we use the expressions below:

$$\varphi^a(\rho) = f(\rho) \begin{pmatrix} \cos(\phi) \\ \sin(\phi) \\ 0 \end{pmatrix}, \quad (14)$$

$$\chi^a(\rho) = g(\rho) \begin{pmatrix} -\sin(\phi) \\ \cos(\phi) \\ 0 \end{pmatrix}, \quad (15)$$

$$\vec{A}^a(\rho) = \hat{\phi} \left( \frac{1 - H(\rho)}{\epsilon \rho} \right) \delta_{a,3} = -\hat{\phi} \frac{A(\rho)}{\epsilon \rho} \delta_{a,3} \quad (16)$$

and

$$A_t^a(\rho) = 0, \quad a = 1, 2, 3. \quad (17)$$

We can see that both iso-vector bosonic fields satisfy the orthogonality condition,  $\varphi^a \chi^a = 0$ .

### III. EQUATION OF MOTION

In order to present the equations of motion in a more appropriate form to apply numerical analyzes, we shall define new dimensionless variables and functions as shown below:

$$x = \sqrt{\lambda_1} \eta_1 \rho, \quad f(\rho) = \eta_1 X(x), \quad g(\rho) = \eta_1 Y(x) \quad \text{and} \quad L(x) = \sqrt{\lambda_1} L(\rho) \eta_1. \quad (18)$$

Therefore, the Lagrangian depends only on dimensionless variables and parameters:

$$\alpha = \frac{e^2}{\lambda_1}, \quad q = \frac{\eta_1}{\eta_2}, \quad \beta_i^2 = \frac{\lambda_i}{\lambda_1}, \quad i = 1, 2, 3, \quad \gamma = \kappa \eta_1^2 \quad \text{and} \quad \kappa = 8\pi G. \quad (19)$$

It is convenient to use the Einstein equation in the form

$$R_{\mu\nu} = -\kappa \left( T_{\mu\nu} - \frac{1}{2} g_{\mu\nu} T \right), \quad \text{with} \quad T = g^{\mu\nu} T_{\mu\nu} \quad \text{and} \quad \mu, \nu = t, x, \phi, z. \quad (20)$$

The energy-momentum tensor associated with the mater field is defined by,

$$T_{\mu\nu} = \frac{2}{\sqrt{-g}} \frac{\delta S}{\delta g^{\mu\nu}}, \quad g = \det(g_{\mu\nu}). \quad (21)$$

Varying the action (1) with respect to matter fields and metric tensor, we obtain a system of five non-linear coupled differential equations. The Euler-Lagrange equations are:

$$\frac{(N^2 L X')'}{N^2 L} = X \left[ X^2 - 1 + \beta_3^2 (Y^2 - q^2) + \frac{H^2}{L^2} \right], \quad (22)$$

$$\frac{(N^2 L Y')'}{N^2 L} = Y \left[ \beta_3^2 (X^2 - 1) + \beta_2^2 (Y^2 - q^2) + \frac{H^2}{L^2} \right], \quad (23)$$

$$\frac{L}{N^2} \left( \frac{N^2 H'}{L} \right)' = \alpha (X^2 + Y^2) H. \quad (24)$$

As to the Einstein equations (20), we obtain:

$$\frac{(L N N')'}{N^2 L} = \gamma \left[ \frac{H'^2}{2\alpha L^2} - \frac{1}{4} (X^2 - 1)^2 - \frac{\beta_2^2}{4} (Y^2 - q^2)^2 - \frac{\beta_3^2}{2} (X^2 - 1) (Y^2 - q^2) \right] \quad (25)$$

and

$$\frac{(N^2 L')'}{N^2 L} = -\gamma \left[ \frac{H'^2}{2\alpha L^2} + (X^2 + Y^2) \frac{H^2}{L^2} + \frac{1}{4} (X^2 - 1)^2 + \frac{\beta_2^2}{4} (Y^2 - q^2)^2 + \frac{\beta_3^2}{2} (X^2 - 1) (Y^2 - q^2) \right]. \quad (26)$$

The primes in the above equations denote derivatives with respect to  $x$ .

At this point we would like to notice that the set of differential equation above, Eq.s (22)-(26), reduces itself to the corresponding one for the Abelian Higgs model [10], by taking  $\beta_2 = \beta_3 = 0$  and setting one of the Higgs field equal to zero. Because one of our objective is to compare our results with the corresponding one for the Abelian case, we shall take, when necessary, the bosonic field  $\chi = 0$ , which, in terms of dimensionless functions, corresponds to take  $Y = 0$ .

### A. Boundary conditions

The requirements of regularity at the origin and topologically stable solutions, leads to the following boundary conditions for the matter and gauge fields

$$H(0) = 1; \quad H(\infty) = 0, \quad (27)$$

$$X(0) = 0, \quad X(\infty) = 1, \quad Y(0) = 0, \quad Y(\infty) = \frac{\eta_2}{\eta_1} = q \quad (28)$$

and for the metric fields

$$N(0) = 1, \quad N'(0) = 0, \quad L(0) = 0, \quad L'(0) = 1. \quad (29)$$

The energy density per unity of lenght is given by:

$$\varepsilon = \int \sqrt{{}^{(3)}g} T_t^t d\rho d\phi, \quad (30)$$

where  ${}^{(3)}g$  is the determinant of the (2+1) dimensional metric given in (10) by taking  $dz = 0$ , and  $T_0^0$  is the 00-component of the energy-momentum tensor. Therefore,

$$\begin{aligned} \varepsilon = 2\pi\eta_1^2 \int_0^\infty NL & \left[ \frac{H'^2}{2\alpha L^2} + \frac{1}{2} (X'^2 + Y'^2) + \frac{1}{2} (X^2 + Y^2) \frac{H^2}{L^2} + \frac{1}{4} (X^2 - 1)^2 \right. \\ & \left. + \frac{\beta_2^2}{4} (Y^2 - q^2)^2 + \frac{\beta_3^2}{2} (X^2 - 1) (Y^2 - q^2) \right] dx. \end{aligned} \quad (31)$$

The  $T_\rho^\rho$  and  $T_\phi^\phi$  components are, respectively,

$$\begin{aligned} T_\rho^\rho = \eta_1^4 \lambda_1 & \left[ -\frac{H'^2}{2\alpha L^2} - \frac{1}{2} (X'^2 + Y'^2) + \frac{1}{2} (X^2 + Y^2) \frac{H^2}{L^2} + \frac{1}{4} (X^2 - 1)^2 \right. \\ & \left. + \frac{\beta_2^2}{4} (Y^2 - q^2)^2 + \frac{\beta_3^2}{2} (X^2 - 1) (Y^2 - q^2) \right], \end{aligned} \quad (32)$$

$$\begin{aligned} T_\phi^\phi = \eta_1^4 \lambda_1 & \left[ -\frac{H'^2}{2\alpha L^2} + \frac{1}{2} (X'^2 + Y'^2) - \frac{1}{2} (X^2 + Y^2) \frac{H^2}{L^2} + \frac{1}{4} (X^2 - 1)^2 \right. \\ & \left. + \frac{\beta_2^2}{4} (Y^2 - q^2)^2 + \frac{\beta_3^2}{2} (X^2 - 1) (Y^2 - q^2) \right] \end{aligned} \quad (33)$$

and  $T_z^z = T_t^t$ .

#### IV. NUMERICAL RESULTS

In the following we shall analyze our system. To do that we integrate numerically the equations (22) - (26) with boundary conditions (27 - 29) by using the ODE solver COLSYS [15]. Relative errors of the functions are typically on the order of  $10^{-8}$  to  $10^{-10}$  (and sometimes even better).

As we have said, our objective in this section is to analyze numerically the behavior of the solutions of the non-Abelian gravitating string by specifying the set of physical parameters of the system; moreover, we are also interested to compare these behaviors with the corresponding one for the Abelian gravitating strings, observing, separately, the influence of each system on the geometry of the spacetime.

Let us first analyze the behaviors of the Higgs and gauge fields besides the metric functions for the non-Abelian string system. In order to do that we construct the plots of these fields as functions of the dimensionless variable,  $x$ . Our results are exhibited in Fig. 1. In the left panel we present the behaviors of the Higgs,  $X$  and  $Y$ , and gauge fields,  $H$ , considering  $\alpha = 1.0$ ,  $\gamma = 0.6$ ,  $\beta_2 = 2.0$ ,  $\beta_3 = 1.0$  and  $q = 1$ . The behaviors of the metric fields,  $N$  and  $L$ , are exhibited in the right panel.

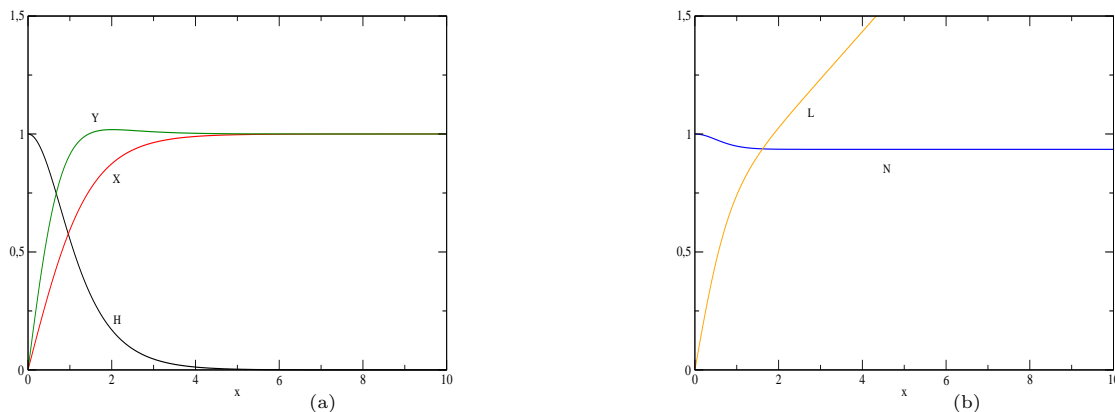


FIG. 1: **Non-Abelian strings:** In the left panel we present the behavior for the Higgs and gauge fields as functions of  $x$  considering the parameters  $\alpha = 1.0$ ,  $\gamma = 0.6$ ,  $\beta_2 = 2.0$ ,  $\beta_3 = 1.0$  and  $q = 1.0$ . In the right panel we present the behavior of the metric functions.

Concerning now the behaviors of the matter, gauge fields and the metric functions for the Abelian string, we adopt the procedure already explained. So, we plot the fields  $X$  and  $H$ , besides the metric fields,  $L$  and  $N$ , as functions of  $x$ . In the the left panel of Fig. 2 we present the behaviors for the Higgs and gauge fields considering  $\alpha = 1.0$  and  $\gamma = 0.6$ . The corresponding behaviors for the metric functions are shown in the right panel.

The comparison of the behaviors for the metric functions,  $L$  and  $N$ , as functions of  $x$  for both, non-Abelian and Abelian strings, are exhibited in Fig. 3, considering  $\alpha = 1.0$ ,  $\gamma = 0.6$ ,  $\beta_2 = 2.0$ ,  $\beta_3 = 1.0$  and  $q = 1.0$  for the non-Abelian string and  $\alpha = 1.0$ ,  $\gamma = 0.6$  for the Abelian string.

Both, non-Abelian and Abelian string solutions, provide planar angle deficit in the corresponding spacetime. This quantity is given by analyzing the slop of  $L$  for points very far from the string's core. The planar angle deficit is given by:

$$\delta = 2\pi(1 - L'(\infty)) . \quad (34)$$

Moreover, the linear energy density is obtained by integrating (31). Taking for the parameters the values used in the previous plots, we have found for the planar angle deficits and energy densities per unity of  $2\pi\eta_1^2$ , respectively, the following results:

$$\delta_{NA} \approx 0.7998 \text{ and } \delta_A \approx 0.3493 \quad (35)$$

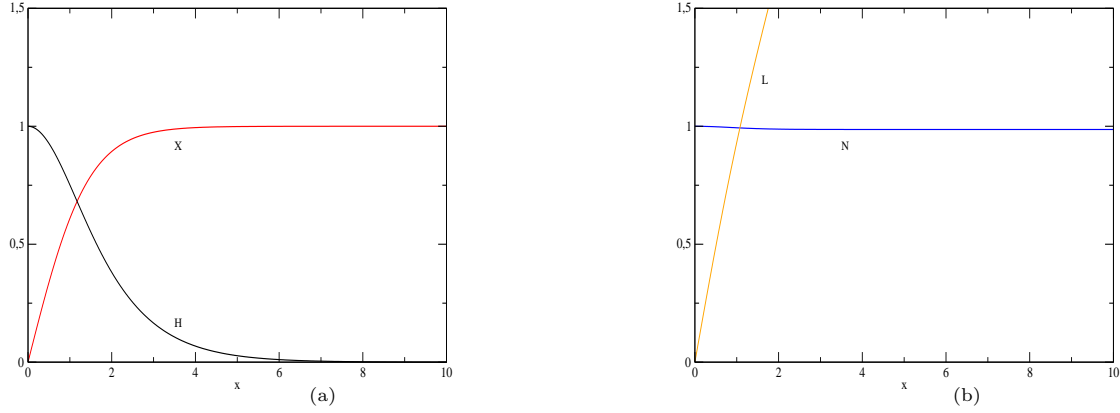


FIG. 2: **Abelian strings:** In the left panel we present the behavior for the Higgs and gauge fields as functions of  $x$ , considering the parameters  $\alpha = 1.0$ ,  $\gamma = 0.6$ . In the right panel, we present the behavior of the metric functions.

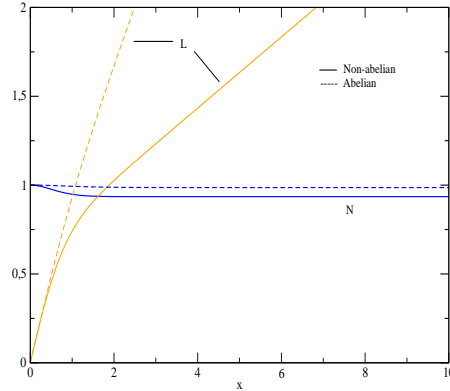


FIG. 3: This figure shows the comparison between the behavior of the metric functions as functions of  $x$ , considering  $\alpha = 1.0$ , and  $\gamma = 0.6$ . For the non-Abelian case, we have taken  $\beta_2 = 2.0$ ,  $\beta_3 = 1.0$  and  $q = 1.0$ .

and<sup>2</sup>

$$\varepsilon_{NA}/(2\pi\eta_1^2) \approx 1.2856 \text{ and } \varepsilon_A/(2\pi\eta_1^2) \approx 1.1646. \quad (36)$$

Another relevant analysis associated with the non-Abelian strings concerns the behavior of their energy densities. Two independent analysis have developed by us: The energy density per units of  $2\pi\eta_1^2$  as function of  $\beta_3$  and  $\gamma$ . In the left panel of the Fig. 4, we exhibit this behavior as function of  $\beta_3$  considering  $\gamma = 0.6$ . In the right panel we present this behavior as function of  $\gamma$  considering  $\beta_3 = 1.0$ . For both plots we have taken  $\alpha = 1.0$ ,  $\beta_2 = 2.0$  and  $q = 1$ .

The behaviors of the planar angle deficit in units of  $2\pi$ ,  $\delta/2\pi$ , as function of  $\beta_3$  and  $\gamma$ , are presented in Fig. 5. In the left plot we present  $\delta/2\pi$  as function of  $\beta_3$  considering  $\gamma = 0.6$ . In the right plot we present this behavior as function of  $\gamma$  considering  $\beta_3 = 1.0$ . For both plots we have taken  $\alpha = 1.0$ ,  $\beta_2 = 2.0$  and  $q = 1$ .

<sup>2</sup> The sub-scripts  $NA$  and  $A$  refer to the non-Abelian and Abelian strings, respectively.

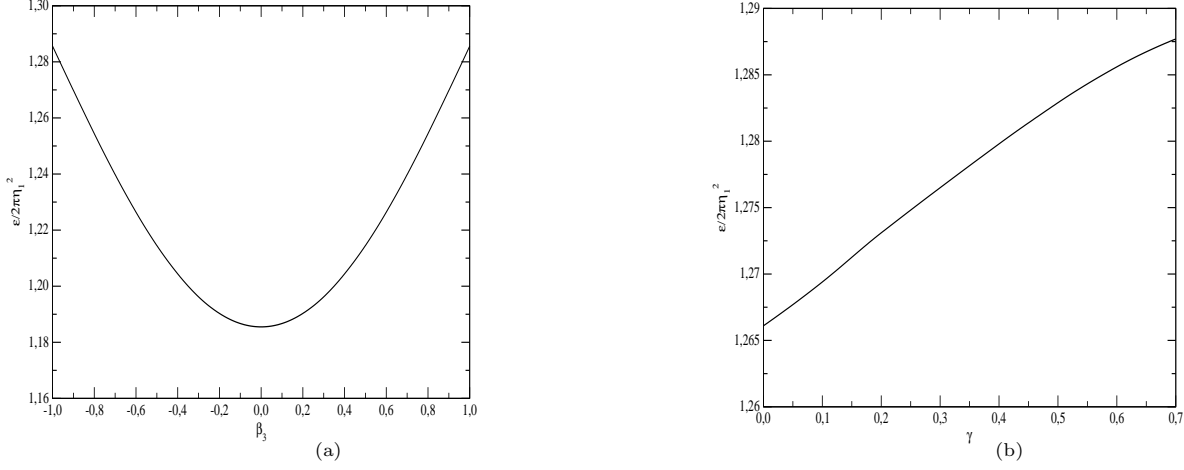


FIG. 4: In the left panel we present the behavior of the energy density per unit of  $2\pi\eta_1^2$  as function of  $\beta_3$  considering  $\gamma = 0.6$ . In the right panel we present the behavior of the energy density per unit of  $2\pi\eta_1^2$  as function of  $\gamma$ , considering  $\beta_3 = 1.0$ . In both graphs we have taken  $\alpha = 1.0$ ,  $\beta_2 = 2.0$  and  $q = 1$ .

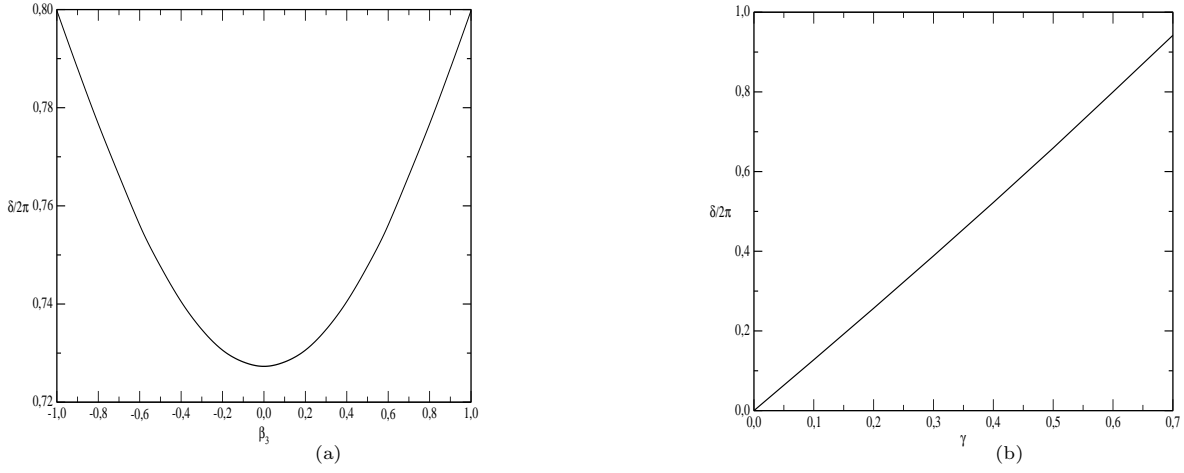


FIG. 5: In the left plot we present the behavior of the the planar angle deficit in units of  $2\pi$  as function of  $\beta_3$  considering  $\gamma = 0.6$ . In the right plot we present this behavior as function of  $\gamma$ , considering  $\beta_3 = 1.0$ . In both plots we have taken  $\alpha = 1.0$ ,  $\beta_2 = 2.0$  and  $q = 1$ .

The solutions that we are analyzing in this paper, named regular strings, are the ones that present the planar angle deficit,  $\delta$ , smaller than  $2\pi$ . The planar angle deficit is a measurement of the the modification on the geometry of the spacetime caused by gravitational interaction of the system. To obtain regular strings is required an optimal choice of the parameters  $\alpha$ ,  $\gamma$ ,  $\beta_2$ ,  $\beta_3$  and  $q$ . For fixed values of  $\beta_2$ ,  $\beta_3$  and  $q$ , it is possible to determine regular solutions examining the region below the curve in the  $(\alpha - \gamma)$  parameter space. However, from equation (31), the energy density



decreases as  $\alpha$  is increased. Moreover, as shown in the Fig. 4(b), the energy density increases with  $\gamma$ . Therefore, regular strings are obtained until the critical value of  $\gamma$  is achieved,  $\gamma_{cr}$ . This  $\gamma_{cr}$  is described by the curve in the  $(\alpha - \gamma)$  parameter space. If  $\beta_3 = 0.0$ ,  $\gamma_{cr}$  is greater than in the case of  $\beta_3 \neq 0.0$  because there is no contribution to energy density from the coupled bosonic sectors. This fact is showed in Fig. 6, where we have considered  $\beta_2 = 2.0$  and  $q = 1$ , for  $\beta_3 = 0.0$  and  $1.0$ .

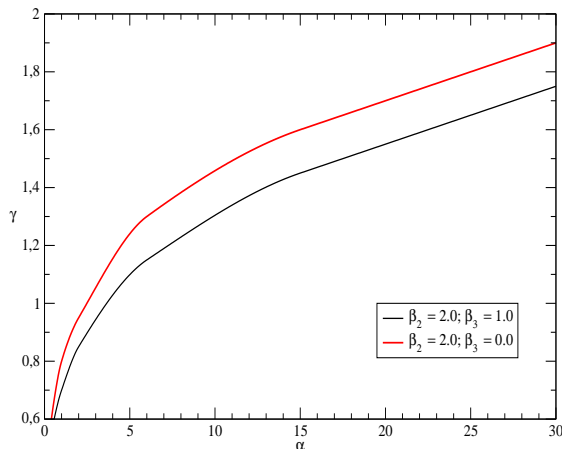


FIG. 6: This figure shows the the regions in the  $(\alpha - \gamma)$  parameter space, which contains regular non-Abelian string solutions. Our plots were developed considering two distinct values of  $\beta_3$  (see the graph). For both cases, we consider  $q = 1.0$  and  $\beta_2 = 2.0$ .

## V. CONCLUSION

In this paper we have investigated gravitating non-Abelian,  $SU(2)$ , Higgs model of cosmic strings. In order to have non-Abelian stable topological string it is necessary the presence of two bosonic iso-vectors. As to the interaction potential, besides contains forth power terms in the fields, it may present a direct coupling interaction between the bosonic sectors. The numerical analysis were developed considering specific values of the physical parameters of the model.

One of our objective was to compare the behaviors of the metric functions corresponding to the non-Abelian and Abelian gravitating strings as function of the dimensionless variable,  $x$ . These behaviors were exhibited, separately, in Fig. 1 and Fig. 2. In Fig 3, we have displayed the behavior of the metric functions,  $N$  and  $L$ , for both strings. We can notice that, for specific values of the parameter<sup>3</sup>, the non-Abelian string provides a larger planar angle deficit than the corresponding Abelian one, although the corresponding energy density is larger. In fact, by our results, the planar angle deficit is approximately 2.290 bigger and the corresponding energy density is also bigger, approximately 1.104.

As to the non-Abelian string, we have analyzed the behavior of the energy density as function of  $\beta_3$  and  $\gamma$ . In figure 4(a) we can observe that its minimum value occurs for  $\beta_3 = 0$ , and in the figure 4(b) we see that the energy density increases with  $\gamma$ .

The analysis of the planar angle deficit as function of  $\beta_3$  and  $\gamma$  are exhibited in Fig. 5. In the figure 5(a) we can see that the minimum value for this quantity happens for  $\beta_3 = 0$ ; of course, in this analysis, it is necessary that  $\gamma > 0$ .

We have also provided in Fig. 6, a graph that exhibit a region in the  $(\alpha - \gamma)$  parameter space where regular strings can be formed for  $\beta_2 = 2.0$  and  $q = 1$  for two specific values of  $\beta_3$ . This region is below the curved line in the plot. As we can see, considering  $\beta_3 = 0$ , for a given  $\alpha$  the critical value for  $\gamma$  which allows regular string is bigger than for

<sup>3</sup> We have considered  $\alpha = 1.0$  and  $\gamma = 0.6$  for both cases, and  $\beta_2 = 2\beta_3 = 2.0$  and  $q = 1$  for the non-Abelian string.

$\beta_3 = 1$ . This fact is consequence of the dependence of the energy density, Eq. (31), with  $\beta_3$ . Because the planar angle deficit increases with  $\varepsilon$ , the planar angle deficit depends on  $\beta_3$ ; so vanishing this parameter, to attain  $\delta/2\pi$  near unity is required larger value of  $\gamma$ .

In great part of the analysis developed in this paper we have considered parameters that provide  $\Delta > 0$ ; however, in the Appendix, we analyze a special case of non-Abelian string where this condition is not fulfilled. This solution presents some similarity with the BPS solution of the Abelian Higgs string, i.e., it presents the metric function  $N$  equal to unity, and allows to reduce the set of differential equation to a simpler one. We also analyzed in the Appendix the behavior of the BPS Abelian-Higgs string.

**Acknowledgment:** E.R.B.M. would like to acknowledge CNPq for partial financial support. A. de P. S. would like to acknowledge the Universidade Federal Rural de Pernambuco. Also the authors would like to acknowledge Betti Hartmann for her valuable contributions during all steps of this paper.

### Appendix A: The Special Case

As it is well known, the Abelian-Higgs system presents the BPS solution for the fields equation. This solution is characterized by the fact of be solution of a set of first order differential equation which minimize the energy density of the string. This configuration is achieved by taking  $\alpha = 2.0$  in the equations of motion and assuming  $N = 1$  [10]. The BPS limit for the Abelian Higgs model can be obtained from our system of differential equations, by taken  $\beta_2 = \beta_3 = 0$ ,  $\alpha = 2.0$  and assuming the field  $Y = 0$  and the metric function  $N = 1$  equal to the unity. In this case the set of differential equations reduce to:

$$H' = L(X^2 - 1) \ , L'' = -\gamma L \left[ \frac{X^2 H^2}{L^2} + \frac{(X^2 - 1)^2}{2} \right] \quad (\text{A1})$$

and

$$X' = X \frac{H}{L} \ . \quad (\text{A2})$$

Here, for the non-Abelian string case, we wish to analyze a special solution of the fields equation that present characteristic similar to the Abelian BPS one; however, for this case, we have  $\Delta = \lambda_1 \lambda_2 - \lambda_3^2 = 0$ . In order to construct this solution we shall substitute  $\alpha = 2.0$ ,  $\beta_i = 1.0$ ,  $N = 1$  and  $q = 1.0$  into the equations (25) and (26). So, we get:

$$H' = L(X^2 + Y^2 - 2) \quad (\text{A3})$$

and

$$L'' = -\gamma L \left[ (X^2 + Y^2) \frac{H^2}{L^2} + \frac{1}{2} (X^2 + Y^2 - 2)^2 \right] \ . \quad (\text{A4})$$

Moreover, taking  $\alpha = 2.0$  into Eq. (24), two particular independent linear differential equations can be obtained. They are:

$$X' = X \frac{H}{L} \text{ and } Y' = Y \frac{H}{L} \ . \quad (\text{A5})$$

With these conditions, we can verify that the radial and azimuthal components of the energy-momentum tensor vanish:

$$T_\rho^\rho = T_\phi^\phi = 0 \ . \quad (\text{A6})$$

As to the energy density and axial tension, by using equations (A3) to (A5), they can be expressed by:

$$T_z^z = T_t^t = \frac{\eta_1^4 \lambda_1}{2L} [H(X'^2 + Y'^2 - 2)]' \ , \quad (\text{A7})$$

where the derivative is with respect to  $x$ .

Our numerical analysis for both, non-Abelian and Abelian, solutions above mentioned are displayed in Fig. 7. In the left panel, we present the behaviors of the Higgs and gauge fields, and the metric functions, for this special case for the non-Abelian string, considering  $\alpha = 2.0$ ,  $\beta_2 = \beta_3 = 1$  and  $q = 1$ . In the right panel we exhibit the behaviors for the Higgs and gauge fields, and also for the metric functions for the BPS solution of the Abelian strings considering  $\alpha = 2.0$ . For both cases we took  $\gamma = 0.6$ .

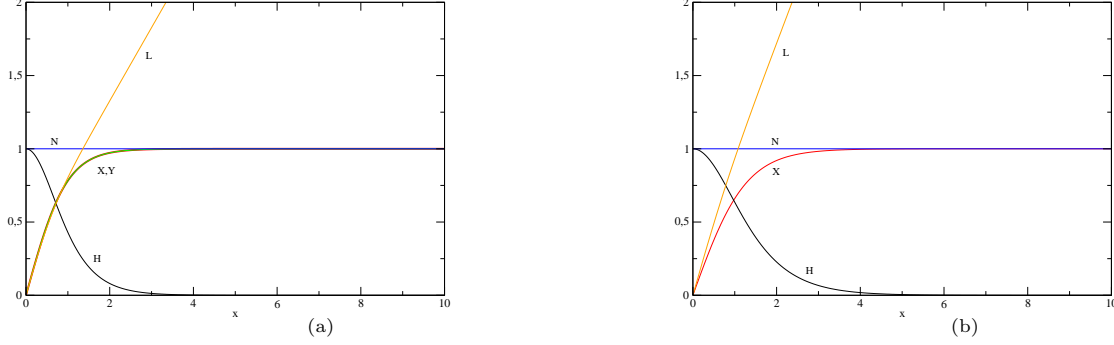


FIG. 7: In the left panel we present the behaviors for the Higgs and gauge fields, and for the metric functions considering  $\gamma = 0.6$ ,  $\alpha = 2.0$ ,  $\beta_2 = \beta_3 = 1$  and  $q = 1$ , for the non-Abelian special case. In the right panel, we present the behaviors of the Higgs and gauge fields, and the metric functions for the Abelian BPS string, considering  $\gamma = 0.6$  and  $\alpha = 2.0$ .

Another point that we want to mention is with respect to the energy per unity length. For both configurations, the energy density per  $2\pi\eta_1^2$  are equal to unity. As to the planar angle deficit it has been shown in [16] that for the Abelian BPS solution,

$$\frac{\delta}{2\pi} = \frac{\gamma}{2} . \quad (\text{A8})$$

For the special case of non-Abelian string, we can show by combining (A3) to (A5) that

$$L'' = -\frac{\gamma}{2} [H(X^2 + Y^2 - 2)]' . \quad (\text{A9})$$

Integrating the above expression we have,

$$L'(\infty) = 1 - \gamma . \quad (\text{A10})$$

Consequently by (34), we obtain,

$$\frac{\delta}{2\pi} = \gamma . \quad (\text{A11})$$

As we can see, although both solutions presents the same energy density, the planar angle deficit associated with the non-Abelian "BPS" configuration is twice bigger than the deficit for the Abelian BPS string. The reason for this fact is because in the non-Abelian "BPS" configuration there are the contribution of two bosonic sectors against just one bosonic sector for the Abelian BPS solution in the definition of the planar angle deficit. Finally we want to mention that our numerical results have exhibited that:

- Both energies density per  $2\pi\eta_1^2$  are equal to unity.
- Both planar angle deficits are in good agreement with the expressions (A8) and (A11).

- [2] A. Vilenkin and E. S. Shellard, *Cosmic strings and others topological defects*. Cambridge University Press (2000).
- [3] **Planck Collaboration** Collaboration, P. Ade et al., *Planck 2013 results XXV. Searches for cosmic strings and other topological defects*, arXiv:1303.5085.
- [4] M. Hindmarsh, *Signals of Inflationary Models with Cosmic Strings*, *Prog. Theor. Phys. Suppl.* **190** (2011) 197-228, arXiv:1106.0391.
- [5] E. J. Copeland, L. Pogosian and T. Vachapati, *Seeking String Theory in the Cosmos*, *Class. Quant. Grav.* **28** (2011) 204009, arXiv:1105.0207.
- [6] H. B. Nielsen and P. Olesen, *Nuclear Physics B* **61**, 45 (1973).
- [7] D. Garfinkle, *Phys. Rev. D* **31** 1323 (1985).
- [8] P. Laguna-Castillo and R. A. Matzner, *Phys. Rev. D* **35** 2933 (1987).
- [9] M. Christensen, A. L. Larsen and Y. Verbin, *Phys. Rev. D*, **60**, 125012, (1999).
- [10] Y. Brihaye and M. Lubo, *Phys. Rev. D*, **62**, 085004, (2000).
- [11] B. Hartmann and J. Urrestilla, *JHEP* 0807 (2008) 006.
- [12] H. J. de Vega, *Phys. Rev. D* **18**, 2932 (1978).
- [13] E. R. Bezerra de Mello, Y. Brihaye and B. Hartmann, *Phys. Rev. D* **67**, 124008 (2003).
- [14] E. R. Bezerra de Mello, Y. Brihaye and B. Hartmann, *Phys. Rev. D* **67**, 045015 (2003).
- [15] U. Ascher, J. Christiansen and R. D. Russel, *Math. Comput.* **33** (1979), 659; *ACM Trans. Math. Softw.* **7** (1981), 209.
- [16] Y. Verbin, *Phys. Rev. D* **59** 105015 (1999).